IOSR Journal of Electrical and Electronics Engineering (IOSR-JEEE)
e-ISSN: 2278-1676,p-ISSN: 2320-3331, Volume 10, Issue 5 Ver. II (Sep – Oct. 2015), PP 116-125
www.iosrjournals.org

A New design of A Hydrogen Fueling Station Powered By Renewable Energy Sources

El-Said A. Othman [*], Sherif K. Nawar [**], Faten H. Fahmy[**],
Abd El-Shafy A. Nafeh[**]

[*]*Faculty of Engineering, Al-Azhar University, Cairo, Egypt.*
[**]*Photovoltaic Cells Department, Electronics Research Institute, National Research Center Building, Giza, Egypt.*

Abstract: *This paper focuses on the combination of wind, photovoltaic (PV), and battery for satisfying a hydrogen fueling station power demand. Wind and PV are the main power sources of the station, while as the wind turbine output power varies with the wind speed and the PV output power varies with irradiance: a battery is integrated with the PV/wind output to satisfy the system performance under all conditions. This research proposes new design of a hydrogen fueling station by using a water cooling system for the hydrogen fueling station, and then fed the hot water to the car wash unit. The new design increases the station's overall efficiency by converting the heat energy (energy dissipation) to useful energy. Optimal sizing of PV/wind hybrid energy sources is proposed by using Homer software. A proposed controller is used for energy management among the energy sources and the load. A simulation model for the hydrogen fueling stations has been developed using MATLAB/Simulink. The simulation shows that the system performance under different conditions has been verified using a load demand profile and real weather data.*

Key words:*Electrolyzers, Fuel cell, Heat exchanger, Photovoltaic, Wind, Battery.*

I. Introduction

The use of fossil fuels is larger than the use of renewable energy for generation of electrical energy until today. However, with decreasing oil reserves in the world, and emissions of greenhouse gases (GHGs) and air pollutants are expected to grow over the present century because of rapidly growing demand for oil, especially in developing countries for this all world research for new alternative power source [1]. The renewable energy sources are the most attractive alternative sources to solve these problems. The energy storage technology that can potentially enhance the use of renewable energy is the hydrogen storage. The hydrogen gas is so much lighter when it compares with the air for this it rises fast and is quickly ejected from the atmosphere.

Thus, the hydrogen as a gas (H_2) is not found by itself on Earth. It is found only in compound form with other elements such as water (H_2O), methane (CH_4), coal, and biomass. It is also an abundant element in the Earth's crust. Hydrogen has the highest energy content of any common fuel by weight. It is one of the most promising alternative fuels for the future because it has the capability of storing energy of high quality, and it is in accordance with a sustainable development. Therefore, H_2has been visualized to become the cornerstone of future energy systems, especially in the transportation sector to charge fuel cell electric vehicles (FCEVs) [2]**.** The aim of this work is to provide a new design of a hydrogen fueling station powered by a renewable energy system consists of a PV, wind turbine and battery.

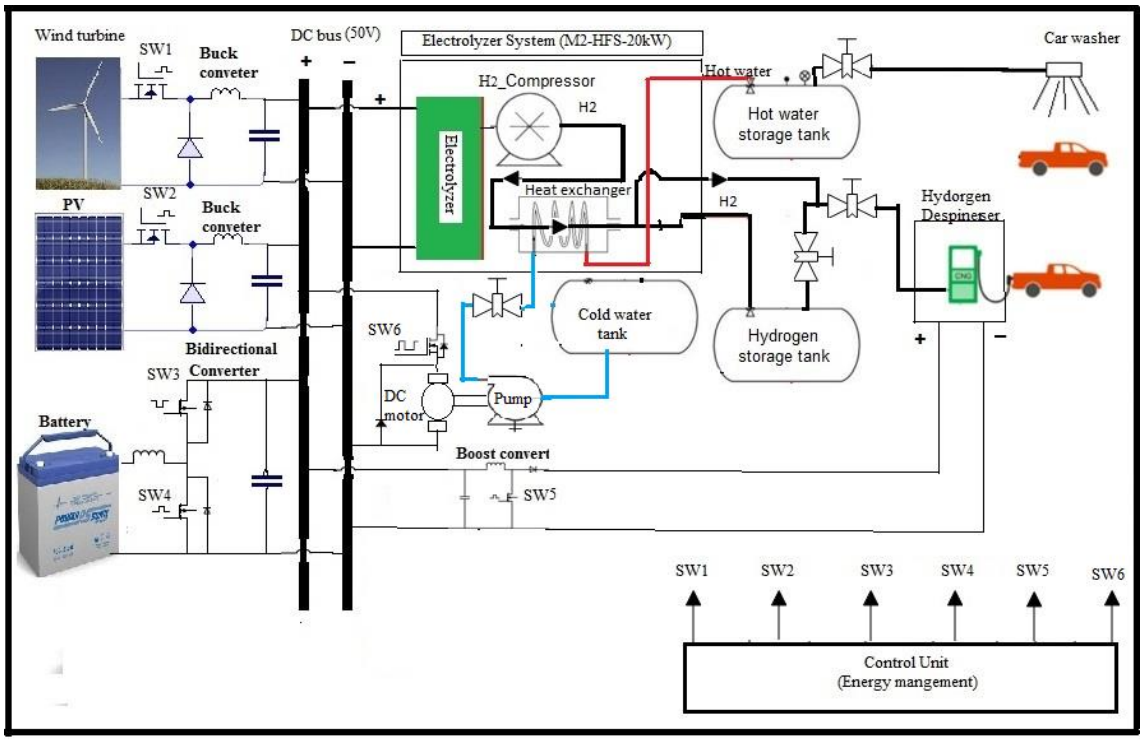

Fig. 1. Schematic diagrams of the proposed hydrogen fueling station.

II. Proposed Hydrogen Fueling Station Configuration

The proposed hydrogen fueling station is shown in Fig. 1. It is shown a 50 volt DC bus to meet the electrolyzer voltage requirement. Each of the PV panel and the wind turbine are connected tot he DC bus through a buck converter. The battery is connected to the DC bus through a bidirectional buck boost converter. Bidirectional converter permits the operation in both directions for battery as the next.

1. The battery delivers power to the load in the case of PV/wind energy sources is less than the required load energy.
2. The battery draws power from the PV/wind energy sources in the case of PV/wind energy sources is larger than the required load energy.

The load on the DC bus is the electrolyzer system (electrolyzer, compressor, and water cooling system). The output of the electrolyzer system is a compressed hydrogen and a hot water both are sent to a hydrogen storage tank and a hot water storage tank respectively.

Control unit used for energy management among all the energy sources and the loads. It is used to drive all the converters and charging and discharging modes of the battery; according to the load requirements and the environmental conditions. Furthermore, it controls the cold water flow rate to reduce electrolyzer system temperature through the heat exchanger.

III. Modeling of the Hydrogen Fueling Station.

In this section, a mathematical models for the hydrogen fueling station subsystems are represented.

3.1. Photovoltaic Model

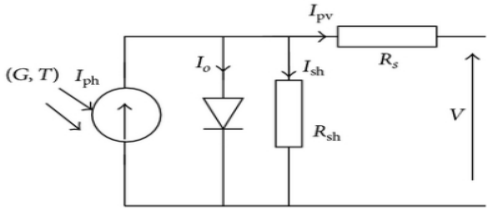

Fig. 2. Equivalent circuit for single-diode model.

The equivalent circuit of PV model is shown in the Fig. 2. DC current is generated when the PV cell is exposed to the solar irradiance. The output I-V and P-V characteristics of a PV cell are nonlinear and vary with

the input solar radiation as well as the cell temperature [3]. The relationship between the current and voltage at the terminals of the PV module is represented by [4].

$$I = I_{ph} - I_o\left[\exp\left(\frac{V + IR_s}{N_s V_t}\right) - 1\right] - \frac{V + IR_s}{R_{sh}} \qquad (1)$$

Where I is the module current, V is the module voltage, I_{ph} is the photo generated current, I_0 is the diode reverse saturation current, R_s is the series resistance, R_{sh} is the shunt resistance, N_s is the number of series connected cells in the module, and V_t is the junction thermal voltage and can be expressed as.

$$V_t = \left(\frac{kAT}{q}\right) \qquad (2)$$

Where k is the Boltzmann's constant equal to 1.38 × 10−23 J/K, q is the electron charge equal to 1.602 × 10−19 C, A is the diode ideality constant, and T is the PV cell temperature.

3.2. Wind Turbine Model

The model of the wind turbine is based on the steady-state power characteristics. The output power of the turbine is given by the following equation [5].

$$P_m = C_p(\lambda, \beta)\frac{\rho A}{2}V_{wind}{}^3 \qquad (3)$$

Where P_m is the Mechanical output power of the turbine (W), C_p is the performance coefficient of the turbine, ρ is the Air density (kg/m^3), A is the Turbine swept area (m^2), V_{wind} is the Wind speed (m/s), λ is the Tip speed ratio of the rotor blade tip speed to wind speed, β is Blade pitch angle (deg).

3.3. BatteryModel

The models of battery useful for the strategic design are based on state of charge (SOC) knowledge. In consequence, a battery model which gives SOC and voltage level is sufficient. If the current is negative battery charge (5) and discharge if the current is positive (6). This model is designed with the values of the charge and discharge impedanceR_{charge}, and $R_{discharge}$ respectively of the battery. Fig. 3 illustrates the electric scheme of the battery model [6, 7].

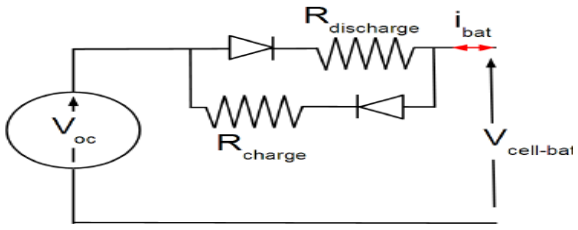

Fig. 3. Battery charge/discharge model.

$$\mathrm{SOC(t)} = \mathrm{SOC(t0)} + (1/3600)\ \mathrm{i_{bat}\ dt} \qquad (4)$$

$$\mathrm{i_{bat}} \le 0 \rightarrow \mathrm{V_{cell-bat}} = \mathrm{Voc} + \mathrm{i_{bat}\ R_{charge}} \qquad (5)$$

$$\mathrm{i_{bat}} \ge 0 \rightarrow \mathrm{V_{cell-bat}} = \mathrm{Voc} - \mathrm{i_{bat}\ R_{discharge}} \qquad (6)$$

Where $V_{cell-bat}$ is the battery cell voltage, i_{bat} is the current of the battery, V_{oc} is the open source voltage.

3.4. Electrolyzer Model

The electrolyzer decomposes the water into hydrogen and oxygen. The total reaction of splitting water isaccording to the Faraday's law is given by [8].

$$H_2O + electrical\ energy \longrightarrow H_2 + 1/2\ O_2 + heat \qquad (7)$$

The hydrogen production rate of the electrolyzer cell is directly proportional to the electrical current. The electrolyzer dynamic model equations can write as [9].

$$n_{H2} = \frac{\eta_F n_c i_e}{2F} \qquad (8)$$

$$\eta_F = 96.5e\left(\frac{0.09}{ie} - \frac{75.5}{ie^2}\right) \qquad (9)$$

Where F is the Faraday constant [C $kmol^{-1}$], i_e is the electrolyzer current [A], n_c is the number of electrolyzer cells in series, $\eta_F$is Faraday efficiency, $n_{H2}$is the hydrogen production [mol s^{-1}].

3.5. Hydrogen Storage Model

The amount of the hydrogen produced by the electrolyzer is sent to the storage tank via compressor. The fundamental equation governing the dynamics of the tank is the law of conservation of mass [13].

$$\frac{dm(t)}{dt} = m_{H2\_i} - m_{H2\_o} \qquad (10)$$

Where m_{H2_i} is the input hydrogen mass flow rate, m_{H2_o} is the output hydrogen mass flow rate, and m(t) is the total mass of hydrogen at time t. The desired output from the hydrogen storage tank model is the hydrogen pressure at time t. By assuming ideal gas behavior and small changes in the air temperature, Equation (10) can be rewritten as [13].

$$\frac{dP_{inst}}{dt} = \frac{\left(m_{H2\_i} - m_{H2\_o}\right).R.T}{V_T} \qquad (11)$$

Where P_{inst} is the instantaneous pressure in the tank, R is the ideal gas constant, T is the average temperature of the hydrogen in the tank, and V_T is the tank volume.

3.6. Compressor Model

The purpose of the compressor is to be able to fill the hydrogen storage tank at the desired pressure (5000 psi) in order to increase storage capacity. The power needed to drive the compressor is given by [12, 13].

$$P_{comp} = \frac{\gamma}{\gamma - 1} R \frac{T}{\eta_c}\left[\left(\frac{P_2}{P_1}\right)^{\frac{\gamma-1}{\gamma}} - 1\right] q_{H2} \qquad (12)$$

Where η_c is the compressor efficiency, q_{H2} is the rate of hydrogen gas flow [mol s^{-1}], γ is the polytropic coefficient (ratio of specific heats=1.41 for hydrogen), R is the gas constant, T is the inlet temperature in this case electrolyzer outlet temperature [K], and P_2, $P_1$is the outlet and inlet pressure [Pa] respectively.

3.7. Water Cooling System

The proposed water cooling system consists of a heat exchanger and a DC pump. In this research, we use a water cooling system. Because the advantages of using water cooling over theair cooling include water's higher specific heat capacity, higher density, and thermal conductivity. This allows water to transmit heat over greater distances with much less volumetric flow and reduced temperature difference. Moreover, the exhahust hot water is used in car wash unit in hydrogen fueling station.

3.7.1. Heat Exchanger

Heat exchangers are devices that used to transfer heat between two or more gases or fluid streams at different temperatures. It is assumed that the inlet cold water temperature is 25 C^o and the outlet hot water is 50 C^o. Heat transfer equation in heat exchangers given by [14].

$$Q = U * A * F * D * \Delta T_{lm} \qquad (13)$$

Where Q is the rate of heat exchange (kJ/h), U is the overall heat transfer coefficient (kJ/m^2.K), A is the heat exchange area (m^2), and ΔT_{lm} is the long mean temperature difference.

$$U = \frac{1}{\frac{1}{h_i}\left(\frac{D_0}{D_i}\right) + \frac{x_w}{K_m}\left(\frac{D_0}{D_i}\right) + \frac{1}{h_0}} \qquad (14)$$

Where X_w is wall thickness, K_m is the thermal conductivity of wall, h_i and h_o are the individual convective heat transfer coefficients in and out of tube respectively, and Di and D_o are the inner and outer diameter respectively.The long mean temperature difference is calculated by [15].

$$\Delta T_{lm} = \frac{\Delta T1 - \Delta T2}{\ln\left(\frac{\Delta T1}{\Delta T2}\right)} \qquad (15)$$

Where $\Delta T_1 and \Delta T_2$ are illustrated in Fig. 4.

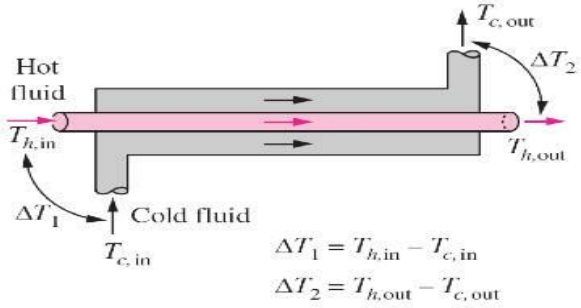

Fig. 4. Heat exchanger temperature difference calculations.

3.7.2. DC Pump

The cold water flow rate is controlled by controlling the speed of the DC motor.The DC motor drives the water circulation pump.The amount of water flow rate is directly related to the amount of heat generated by the electrolyzer system. The DC motor equivalent circuit is shown in Fig.5 and the DC motor equation is given by [16].

$$L_a \frac{di_a}{dt} + R_a . i_a = V_{dc} - E_a \qquad (16)$$

Where $L_a$is the armature inductance, Ra is the armature resistance, i_a is the armature current, Va is the motor applied voltage, and E_a is the induced voltage.

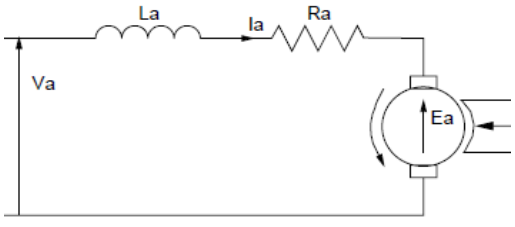

Fig.5. DC motor equivalent circuit

IV. Sizing of PV-Wind Hybrid Energy Source

Hurghada city, Egypt is chosen to become the location of this study because, it is characterized by an intensive solar radiation. Wind is also an abundant resource. The sizing and optimization of the PV-wind hybrid renewable energy source for hydrogen fueling station were performed using HOMER software. HOMER solves the optimization problem to minimize the global cost and provides the optimum PV, wind turbine, and battery size.

4.1. PV and Wind Resources

The profile of the available wind speeds in the Hurghada city as well as solar radiation profile are shown in Figs.6 and 7 [17].

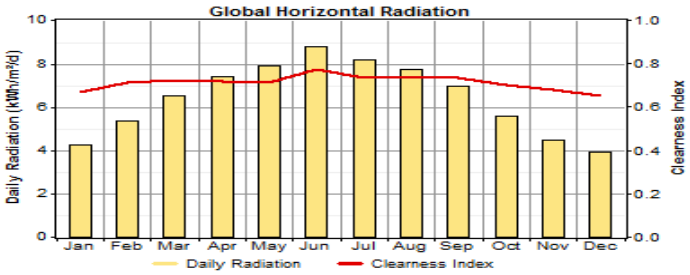

Fig. 6. Averages monthly solar radiation profile of Hurghada city.

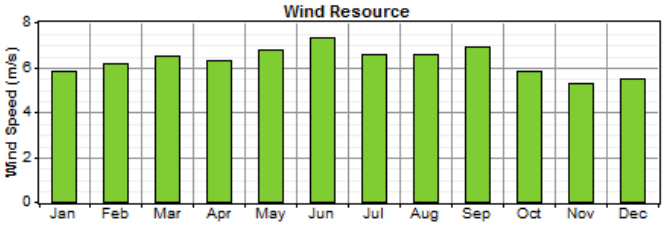

Fig. 7. Averages monthly wind speed Profile for Hurghada city.

4.2. Hydrogen Fueling Station Load Data

The electrolyzer specifications of the proposed hydrogen station are shown in Table 1 [18, 19]. This electrolyzer contains an internal compressor and a heat exchanger. The main load of the hydrogen fueling station is the electrolyzer which is assumed to be operated as shown in Fig. 10. The power of the hydrogen fuel dispenser unitis illustrated in Table 2.

Table 1. Electrolyzer specifications.

Rated power	20kW
Maximum operating power level	20kW
Minimum operating power level	10kW
Hydrogen production rate	0.6 kg/h
Hydrogen fuel quality	99.95%
Operating voltage	50 V DC
Full load current	400 A

Table 2. Hydrogen dispenser unit.

Appliance	No. of units	Power (kW)/unite
Hydrogen fuel dispenser	1	0.75
Flow measurement device	1	0.3

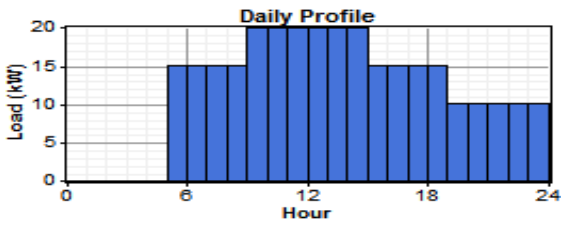

Fig. 8. Daily Load Data of the Hydrogen Fueling Station**.**

4.3. Constraints

The model constraints include:

–The power generated by the hybrid system should meet the demand at any given time.

– Maximum annual capacity shortage is 0%;

– Operating reserve is considered to be 10% of the hourly load.

4.2. Homer Optimization results

The Homer software simulation results of the PV-wind energy source are displayed in Tables 3 and 4. It is observed that the wind power plant has been selected to be three times of the solar power. This is justified due to the cost of wind power installation is less than the PV power instillation, and also the wind speed is Existed a long day, while the solar radiation is existed only from 7 to 10 hours per day. Fig. 9 shows the monthly average electric production of the PV-wind hybrid system.

Table 3. Homer software sizing results

Component	Capital ($)	Replacement ($)	O&M ($)	Fuel ($)	Salvage ($)	Total ($)
PV 11kW	55,000	0	0	0	-5,737	49,263
Wind 31kW	77,500	0	3,011	0	0	80.511
Battery 150kw/h	30,000	30,000	2,914	0	-9,911	53,003
Converter 20kW	14,000	0	1,942	0	0	15,942
System	176,500	30,000	7,867	0	15,648	171,719

Table 4. Energy production per year

Production	kWh/yr	%
PV array	22,395	21
Wind turbines	86,772	79
Total	109,167	100

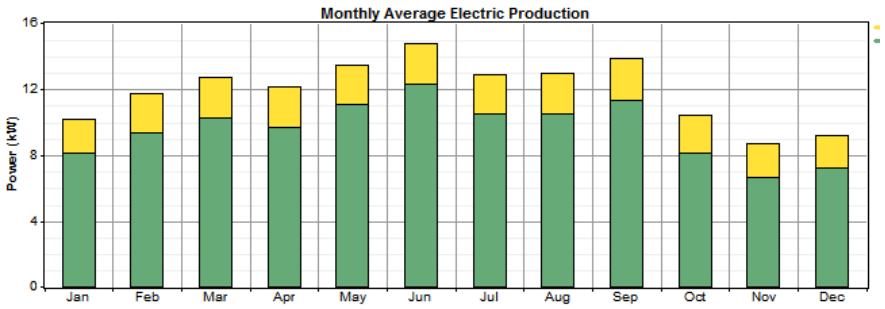

Fig. 9. Monthly average electric production by PV-wind hybrid system.

V. Control strategy

In this section, the proposed control strategy for the fueling station is presented. It is summarized as the next.

1. Power converters are variable structure systems, because of the on/off switching of their IGBTs.
2. The controllers used in the all converters are PI controllers, where they are used to control the converters by sending a PWM to its switches.
3. SW1, SW2, of the two buck converters respectively, are responsible for stabilizing the output voltage of the DC bus voltage at 50 V.
4. SW3, SW4, of the buck-boost bidirectional converter are responsible for charging/discharging the battery.
5. SW5 of the boost converter is used to adjust the dispenser unit voltage at 100 V
6. SW6 of the DC motor driving circuit is used to control the cold water flow rate by varying DC motor speed.

VI. Results and Discussion

In this section, the simulation results for the coupling between the PV/wind /battery and the load are presented. The proposed control strategy can be verified for the following cases: case (I) constant load (at 20 kW), and case (II) step change in the load (initial 10 kW and then 20 kW at t= 5sec). Figs. 10 and 11 show the wind speed and solar insolation variations used for simulation study respectively. Figs. 12 and 13 show the hydrogen fueling station response at constant load, and at step change in the load respectively. As shown in Figs. 12 (a) and 13 (a), the control strategy is capable of regulating the electrolyzer DC bus voltage at 50V. The small spikes in DC voltage caused by the step change in the wind speed and the solar insolation at t= 3 sec and

t= 6sec. The additional spike in DC bus voltage at t= 5sec in Fig. 13 (a) is due to step change in the load at t= 5 sec. The power of the wind, PV, battery and the load are shown in Figs. 12 (b) and 13 (b). From these figures we can notice that the effectiveness of the control unit to meet the load power demand under case (I) and case (II) through control the charge and discharge of the battery. Figs. 12(c) and 13(c) show the state of charge of the battery in case (I) and case (II) respectively. It is clear that the discharge of the battery in case (2) is lower than the case (II) this is because, the average power demands of the load in case (II) is less than the similarities in case (I). The hydrogen production rate of case (I) and case (2) is shown in Figs. 12 (d) and 13 (d) respectively. It is clear that The hydrogen production rate in the case (I) is a constant value 0.6 kg/h due to the electrolyzer has been operated at full power 20 kW, in case (2) the hydrogen production rate is initial 0.3 kg/h and then 0.6 kg/h at t= 5 sec due to the electrolyzer has been operated initially at half power and then skip to full power at t= 5 sec. The controller also appears a good effectiveness in the temperature regulation at 50 C^o through control the flow rate of the cold water in the heat exchanger as shown in Figs. 12 (e) and 13 (e). It is also clear that the rise time of Fig. 12 (d) is lower than the similar in Fig. 13 (d) this because in the case (I) electrolyzer start by full power, which means high current lead to increase the temperature by high rate. Additionally, from Fig. 13 (e) we notice that an additional overshoot in temperature at t= 5 sec this is due to the elctrolyzer skip from half power to full power at this instant. The amount of the cold water flow rate is shown in Figs. 12 (f) and 13 (f).

These figures show the amount of cold water flow rate in case (I) is a constant value 140 L/s, and in case (II) start with 70 L/s and then rise to 140 L/s at t= 5 sec. The amount of the hydrogen stored in the hydrogen storage tank is $1.7e^{-3}$ kg in the case (I) and $1.3e^{-3}$ kg in the case (II) as shown in Figs. 12 (g) and 13 (g) respectively. Also, the hydrogen storage tank pressure is 1.9 psi in case (I) and 1.4 psi in case (II) as shown in Figs. 12 (h) and 13 (h) respectively. It is also clear that the amount of hot water is 2 liter in case (I) and 1.2 litre in case (II) as shown in Figs. 12 (j) and 13 (j) respectively.

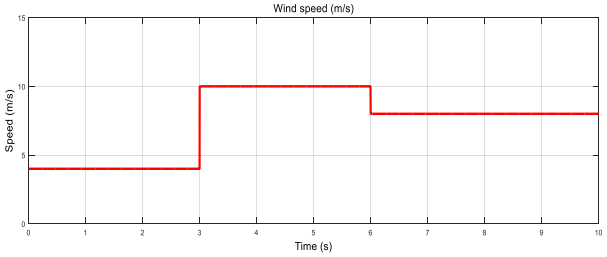

Fig. 10. Wind speed variations used for simulation study.

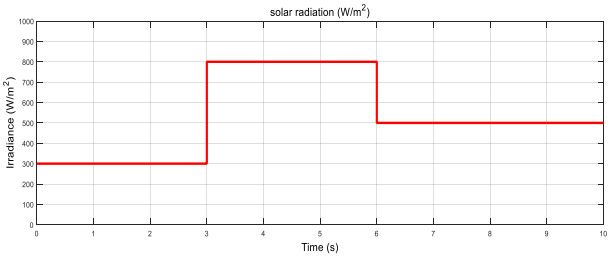

Fig. 11. Wind speed variations used for simulation study.

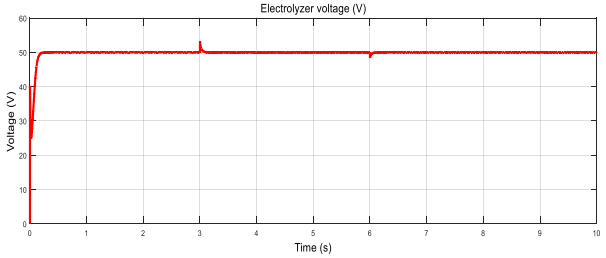

(a) Electrolyzer DC bus voltage

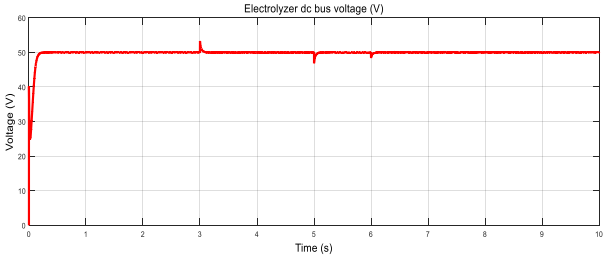

(a) Electrolyzer voltage

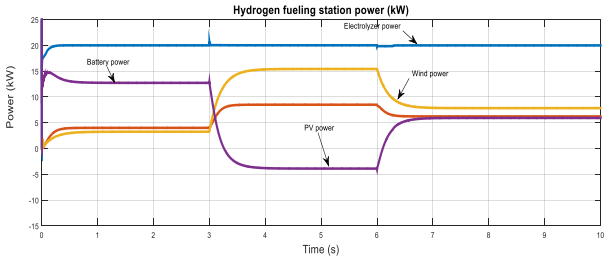

(b) Hydrogen fueling station power

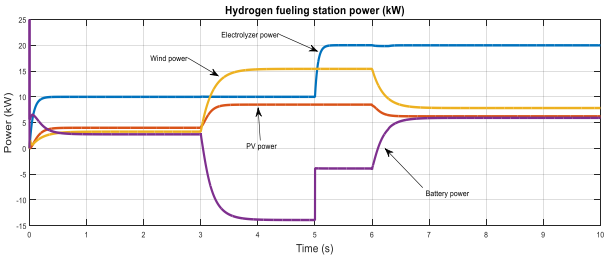

(b) Hydrogen fueling station power

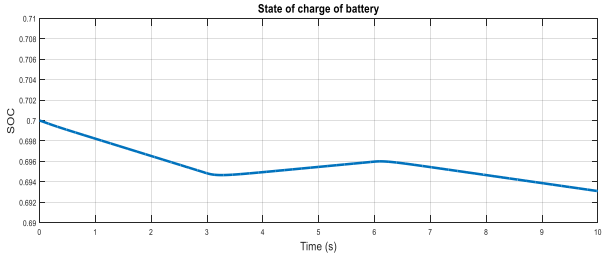

(c) State of charge of battery

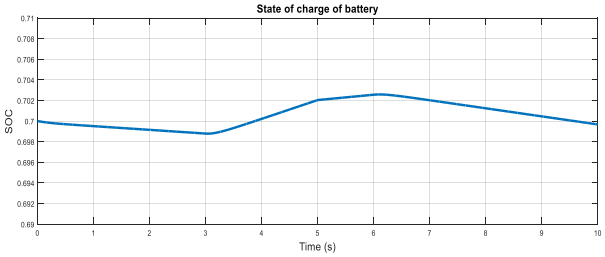

(c) State of charge of battery

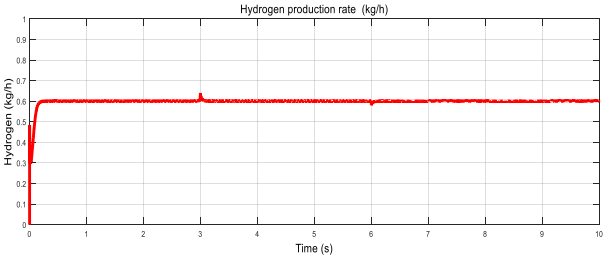

(d) Hydrogen production rate

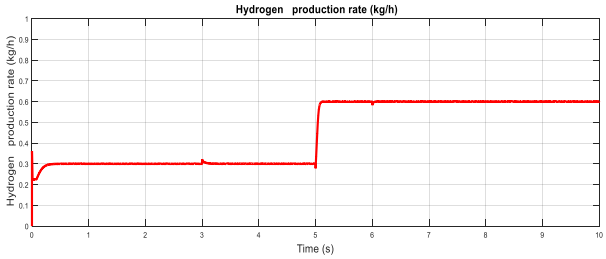

(d) Hydrogen production rate

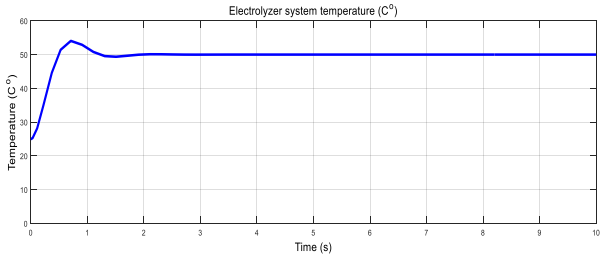

(e) Electrolyzer system temperature

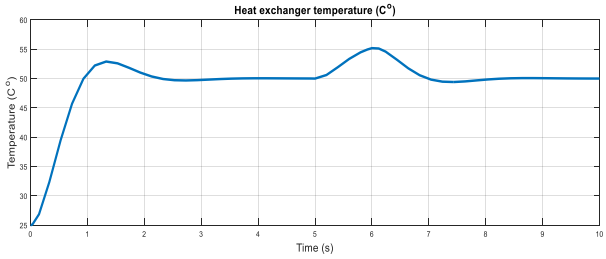

(e) Electrolyzer system temperature

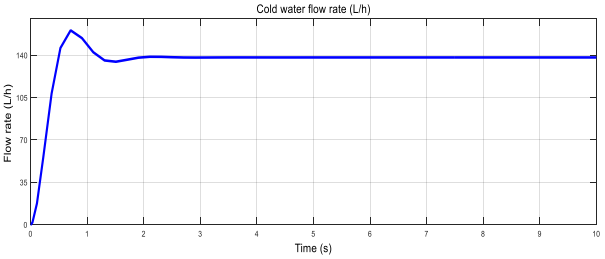

(f) Cold water flow rate

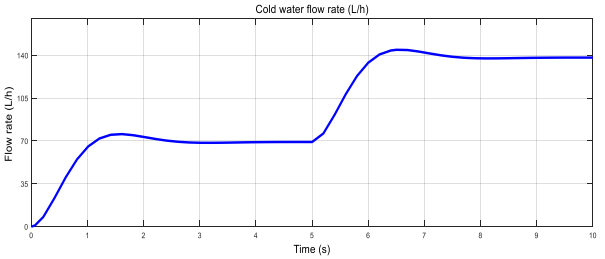

(f) Cold water flow rate

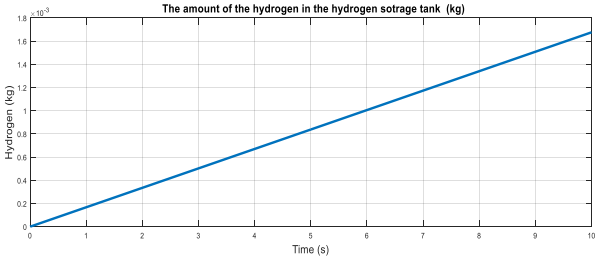

(g) The amount of hydrogen in the hydrogen storage tank

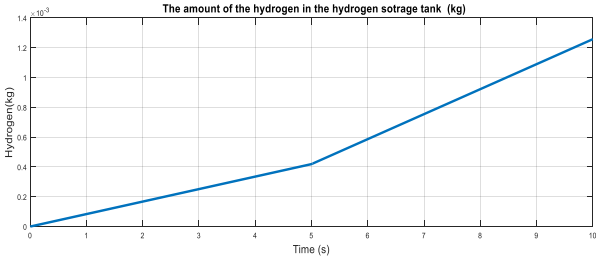

(g) The amount of hydrogen in the hydrogen storage tank

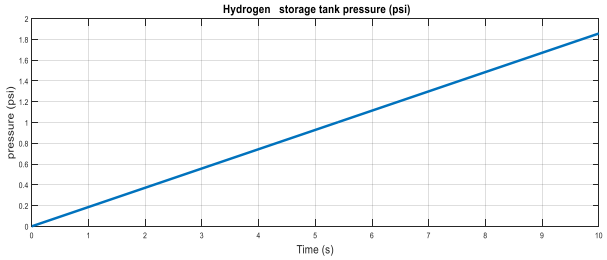

(h) Hydrogen storage tank pressure.

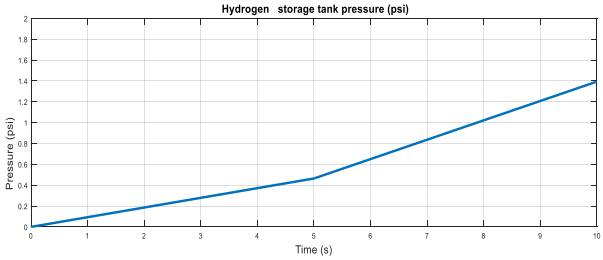

(h) Hydrogen storage tank pressure.

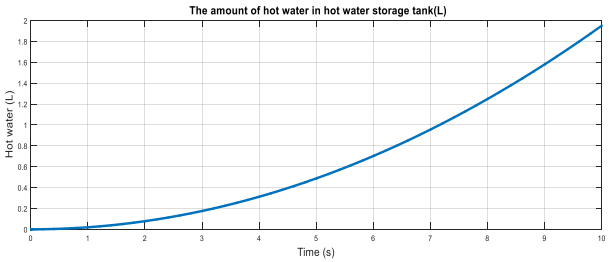

(j) The amount of the hot water in hot tank

Fig. 12. Case(I) Constant load.

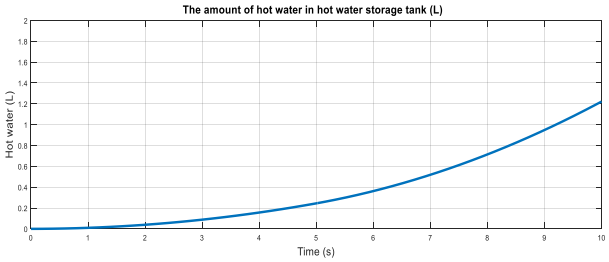

(j) The amount of the hot water in tank

Fig. 13. Case(II) step change in the load.

VII. Conclusion

In this paper, the modelling of all components in a hydrogen fueling station has been developed in order to investigate the dynamic behavior of each subsystem. The optimization problem has been solved using computer pro-gram (HOMER Pro.) to minimize the objective function under the different constraints and provides the optimum wind, solar and battery ratings. Also, this paper introduces an effective control scheme, where the DC voltage regulation and the load power demands has been demonstrated through the MATLAB / SIMULINK.Moreover, a wind/PV/battery/ hybrid power system is designed for a hydrogen fueling station.The electrochemical energy storage systems are found to provide green and clean energy storage for fuel cell electric vehicles and power generation systems.A New design of a hydrogen fueling station is presented by using a water cooling system and then the exhaust hot water of the cooling system is fed to the car wash unit.The station's overall efficiency has been enhanced by this new design.

Reference.

[1] Ogden, Joan M., Robert H. Williams, Eric D. Larson (2004) "Societal Lifecycle Costs of Cars with Alternative Fuels/Engines", Energy Policy 32 (1), 7 – 27.
[2] Mustafa A. Al-Refai, "Matlab/Simulink Simulation of Solar Energy Storage System" International Journal of Electrical, Computer, Electronics and Communication Engineering Vol:8, No:2, 2014.
[3] Huan-Liang Tsai, Ci-Siang Tu and Yi-Jie Su, "Development of Generalized Photovoltaic Model Using Matlab/Simulink," Proceedings of the World Congress on Engineering and Computer Science 2008, pp.1-6, October 2008.
[4] F.Attivissimo,A.DiNisio,M. Savino, and M. Spadavecchia, "Uncertainty analysis in photovoltaic cell parameter estimation," IEEE Trans. Instrum. Meas., vol. 61, no. 5, pp. 1334–1342, May 2012.
[5] E.S. Abdin, W. Xu, Control design and dynamic performance analysis of a wind turbine-induction generator unit, IEEE Trans. Energy Conversion 15 (1) (2000) 91–96.
[6] D. Linden Editor, T. B. Reddy, "Handbook of Batteries", Third Edition,McGraw-Hill, 2002.
[7] Ettihir, K. ; Boulon, L. ; Agbossou, K. ; Kelouwani, S. ; Hammoudi, "M Design of an Energy Management Strategy for PEM Fuel Cell Vehicles", Industrial Electronics (ISIE), 2012 IEEE International Symposium on.
[8] Fuel Cell Handbook, Fifth Ed., EG&G Services Parsons, Inc., 2000.
[9] M.J. Khan, M.T. Iqbal, "Dynamic modeling and simulation of a small wind fuel cell hybrid energy system", J. Renewable Energy 30 (3) (2005) 421–439.
[10] Incropera, F. P. and D. P. DeWitt 2002. Fundamentals of Heat and Mass Transfer. Fifth Edition. John Wiley and Sons, New York, New York.
[11] Rollins, J.P. 1989. Compressed Air and Gas Handbook, Fifth Edition. Prentice Hall, Englewood Cliffs, New Jersey.
[12] James Larminie and Andrew Dicks, Fuel Cell Systems Explained, 2nd Ed. West Sussex, England: Wiley, 2003.
[13] Ø. Ulleberg, "Modeling of advanced alkaline electrolyzers: A system simulation approach," International Journal of Hydrogen Energy, vol. 28, pp. 21-33, 2003.
[14] Middleman, Stanley. An Introduction to Mass and Heat Transfer, Principles of Analysis and Design.Wiley, Dec 1997.
[15] Kakac, S. and Liu, H., Heat Exchangers: Selection, Rating, and Thermal Performance, 1998, CRC Press, Boca Raton, FL.
[16] Austin Hughes, Electric Motors and Drives, Fundamentals, Types and Applications, Third Edition, Newnes, Inc., 2006.
[17] New and Renewable Energy Authority, Ministry of Electricity and Energy, Egyptain Solar Radiation Atlas, Cairo, Egypt, 1998.
[18] http://www.ahasvc.org/page110.html.
[19] http://www.americanhydrogenassociation.org/.and act as an alternate fuel